

Fermion pairing with spin-density imbalance in an optical lattice

This article has been downloaded from IOPscience. Please scroll down to see the full text article.

2006 New J. Phys. 8 179

(<http://iopscience.iop.org/1367-2630/8/9/179>)

View [the table of contents for this issue](#), or go to the [journal homepage](#) for more

Download details:

IP Address: 38.107.179.210

The article was downloaded on 20/02/2012 at 15:23

Please note that [terms and conditions apply](#).

Fermion pairing with spin-density imbalance in an optical lattice

T Koponen¹, J Kinnunen¹, J-P Martikainen², L M Jensen¹
and P Törmä¹

¹ Department of Physics, Nanoscience Center, PO Box 35,
FI-40014 University of Jyväskylä, Finland

² Department of Physical Sciences, PO Box 64,
FI-00014 University of Helsinki, Finland

E-mail: timo.koponen@phys.jyu.fi

New Journal of Physics **8** (2006) 179

Received 7 May 2006

Published 5 September 2006

Online at <http://www.njp.org/>

doi:10.1088/1367-2630/8/9/179

Abstract. We consider pairing in a two-component atomic Fermi gas, in a three-dimensional optical lattice, when the components have unequal densities, i.e. the gas is polarized. We show that a superfluid where the translational symmetry is broken by a finite Cooper pair momentum, namely a Fulde-Ferrel-Larkin-Ovchinnikov (FFLO)-type state, minimizes the Helmholtz free energy of the system. We demonstrate that such a state is clearly visible in the observable momentum distribution of the atoms, and analyse the dependence of the order parameter and the momentum distribution on the filling fraction and the interaction strength.

Contents

1. Introduction	2
2. Theory	3
2.1. Self-consistent equations for Δ , μ_{\uparrow} and μ_{\downarrow}	5
2.2. Experimental parameters	6
3. Free energy analysis	6
3.1. Fixed chemical potentials, $\mathbf{q} = 0$	6
3.2. Fixed numbers of particles, $\mathbf{q} = 0$	8
4. FFLO states	9
5. Conclusions	17
Acknowledgments	17
References	17

1. Introduction

Newly realized strongly interacting Fermi gases [1]–[9] have enabled an intriguing line of research into the nature of fermion superfluidity. In ultra-cold degenerate gases, the system is composed of atoms in different internal states. The number of atoms in different states can be experimentally controlled and this has enabled first experimental studies of polarized trapped Fermi gases [10]–[12]. Imbalanced atomic gases have recently inspired a number of theoretical works [13]–[26], in addition to the wide literature on fermion pairing with unequal chemical potentials or number densities in the fields of condensed matter, nuclear and high-energy physics (for a review of some of these studies, see [27]).

While several parameters of a harmonically trapped Fermi gas can be controlled experimentally, the inhomogeneity is often crucial and some parameters, such as the atomic mass, cannot be changed. The use of optical lattices provides unprecedented tunability and, for example, the effective masses of atoms can be changed by simply changing the laser intensities. Furthermore, in the centre of the optical lattice the effects due to the harmonic trapping can be weak. This versatile tool has been recently widely used and has enabled, among other things, the observation of the superfluid-Mott insulator quantum phase transition [28] in a cloud of bosons. Use of optical lattices is not restricted by quantum statistics and indeed fermions have been studied experimentally in one-dimensional [29, 30] as well as in three-dimensional [31]–[33] optical lattices. In addition, the first experimental results of Bose–Fermi mixtures in optical lattices were recently reported [34].

In this paper, we investigate the properties of polarized Fermi gases in a three-dimensional optical lattice. In particular, we focus on the states of constant density and compare in detail the energetics of the breached pair (BP) states [35]–[38] and the simplest variant of the Fulde–Ferrel–Larkin–Ovchinnikov (FFLO) states [39, 40] in a three dimensional optical lattice. We find that, while the nonzero gap BP state can be a minimum of the Helmholtz free energy, it can lower its energy by forming pairs with nonzero momentum.

We show that the lattice dispersion causes a different dependence of the superfluid gap on the polarization compared to homogeneous systems. We find that, while the nonzero gap BP state can be a minimum of the Helmholtz free energy, it can lower its energy by breaking the

translational symmetry and forming pairs with nonzero momentum as in FFLO states. Section 2 reviews the theory used in the numerical calculations. In section 3, we discuss the free energy analysis and explain, illustrated by numerical examples, why it is necessary to use the Helmholtz free energy in case of a system isolated from the environment with respect to particle exchange, as is the case with trapped atoms. In section 4, we present the results on the FFLO states: we analyse the system behaviour as a function of the lattice filling fraction and the interaction strength between the two pairing components. Furthermore, we present the momentum distribution of the atoms, showing that this easily observable quantity carries a clear signature of the FFLO state. We conclude by a discussion in section 5.

2. Theory

The microscopic Hamiltonian for fermions of two (pseudo) spins \uparrow and \downarrow , in an external potential $V(\mathbf{x})$, is

$$H = \sum_{\sigma} \int \psi_{\sigma}^{\dagger}(\mathbf{x}) \left(-\frac{\hbar^2}{2m} \nabla^2 + V(\mathbf{x}) \right) \psi_{\sigma}(\mathbf{x}) d^3\mathbf{x} + 4\pi\hbar^2 \frac{a}{m} \int \psi_{\uparrow}^{\dagger}(\mathbf{x}) \psi_{\downarrow}^{\dagger}(\mathbf{x}) \psi_{\downarrow}(\mathbf{x}) \psi_{\uparrow}(\mathbf{x}) d^3\mathbf{x}, \quad (1)$$

where a is the s -wave scattering length. With a sufficiently deep periodic potential, the atoms are localized in the minima of the potential, and the system can be described by the Fermi–Hubbard Hamiltonian [41],

$$H - \mu_{\uparrow} N_{\uparrow} - \mu_{\downarrow} N_{\downarrow} = - \sum_{\mathbf{n}} (\mu_{\uparrow} \hat{c}_{\uparrow\mathbf{n}}^{\dagger} \hat{c}_{\uparrow\mathbf{n}} + \mu_{\downarrow} \hat{c}_{\downarrow\mathbf{n}}^{\dagger} \hat{c}_{\downarrow\mathbf{n}}) + U \sum_{\mathbf{n}} \hat{c}_{\uparrow\mathbf{n}}^{\dagger} \hat{c}_{\downarrow\mathbf{n}}^{\dagger} \hat{c}_{\downarrow\mathbf{n}} \hat{c}_{\uparrow\mathbf{n}} - \left(J_x \sum_{\langle \mathbf{n}, \mathbf{m} \rangle_x} + J_y \sum_{\langle \mathbf{n}, \mathbf{m} \rangle_y} + J_z \sum_{\langle \mathbf{n}, \mathbf{m} \rangle_z} \right) (\hat{c}_{\uparrow\mathbf{m}}^{\dagger} \hat{c}_{\uparrow\mathbf{n}} + \hat{c}_{\downarrow\mathbf{m}}^{\dagger} \hat{c}_{\downarrow\mathbf{n}}). \quad (2)$$

Here, $\langle \mathbf{n}, \mathbf{m} \rangle_x$ means a nearest neighbour pair in the x -direction. In mean-field theory, the interaction term in the Hamiltonian is approximated with

$$U \sum_{\mathbf{n}} \hat{c}_{\uparrow\mathbf{n}}^{\dagger} \hat{c}_{\downarrow\mathbf{n}}^{\dagger} \hat{c}_{\downarrow\mathbf{n}} \hat{c}_{\uparrow\mathbf{n}} = U \sum_{\mathbf{n}} (\langle \hat{c}_{\uparrow\mathbf{n}}^{\dagger} \hat{c}_{\downarrow\mathbf{n}}^{\dagger} \rangle \hat{c}_{\downarrow\mathbf{n}} \hat{c}_{\uparrow\mathbf{n}} + \hat{c}_{\uparrow\mathbf{n}}^{\dagger} \hat{c}_{\downarrow\mathbf{n}}^{\dagger} \langle \hat{c}_{\downarrow\mathbf{n}} \hat{c}_{\uparrow\mathbf{n}} \rangle - \langle \hat{c}_{\uparrow\mathbf{n}}^{\dagger} \hat{c}_{\downarrow\mathbf{n}}^{\dagger} \rangle \langle \hat{c}_{\downarrow\mathbf{n}} \hat{c}_{\uparrow\mathbf{n}} \rangle), \quad (3)$$

where the Hartree and Fock terms have been dropped since the former are effectively included in the chemical potentials and the latter do not contribute. A general ansatz $U \langle \hat{c}_{\downarrow\mathbf{n}} \hat{c}_{\uparrow\mathbf{n}} \rangle = \Delta e^{2i\mathbf{q} \cdot \mathbf{n}}$ describes several apparently different states. For equal (pseudo)spin number densities, $\mathbf{q} = 0$ gives the standard Bardeen–Cooper–Schrieffer (BCS) solution. For unequal densities, $\mathbf{q} = 0$ gives the BP solution and nonzero values for \mathbf{q} describe a FFLO state where Cooper pairs have a finite momentum, \mathbf{q} . Finally, $\Delta = 0$ naturally describes a state with no superfluid, i.e. the normal state.

Including the chemical potentials in the Hamiltonian it becomes, in momentum space,

$$H = \frac{1}{M} \sum_{\mathbf{k}} \left((\epsilon_{\mathbf{k}} - \mu_{\uparrow}) \hat{c}_{\uparrow\mathbf{k}}^{\dagger} \hat{c}_{\uparrow\mathbf{k}} + (\epsilon_{\mathbf{k}} - \mu_{\downarrow}) \hat{c}_{\downarrow\mathbf{k}}^{\dagger} \hat{c}_{\downarrow\mathbf{k}} + \Delta \hat{c}_{\uparrow\mathbf{q}+\mathbf{k}}^{\dagger} \hat{c}_{\downarrow\mathbf{q}-\mathbf{k}}^{\dagger} + \text{h.c.} - \frac{|\Delta|^2}{U} \right), \quad (4)$$

where M is the number of lattice sites, μ_\uparrow and μ_\downarrow are the chemical potentials of the different spin species and the lattice dispersion is given by

$$\epsilon_{\mathbf{k}} = 2J_x(1 - \cos(k_x d)) + 2J_y(1 - \cos(k_y d)) + 2J_z(1 - \cos(k_z d)). \quad (5)$$

Here, d is the lattice parameter, i.e. the distance between two neighbouring lattice points. The parameter U describes the energy associated with the interaction of the particles, with negative values corresponding to an attractive interaction. The hopping parameter, J is the energy gain corresponding to tunnelling between nearest-neighbour sites. In a lattice, J is essentially the band width. For a more detailed discussion on the parameters J and U , see e.g. [42]. Using the fermionic anticommutators, the Hamiltonian can be rearranged as (note periodic boundary conditions in the k summations)

$$H = \frac{1}{M} \sum_{\mathbf{k}} \left((\epsilon_{\mathbf{k}+\mathbf{q}} - \mu_\uparrow) \hat{c}_{\uparrow\mathbf{k}+\mathbf{q}}^\dagger \hat{c}_{\uparrow\mathbf{k}+\mathbf{q}} - (\epsilon_{-\mathbf{k}+\mathbf{q}} - \mu_\downarrow) (\hat{c}_{\downarrow-\mathbf{k}+\mathbf{q}} \hat{c}_{\downarrow-\mathbf{k}+\mathbf{q}}^\dagger - 1) + \Delta \hat{c}_{\uparrow\mathbf{q}+\mathbf{k}}^\dagger \hat{c}_{\downarrow\mathbf{q}-\mathbf{k}}^\dagger + \Delta^* \hat{c}_{\downarrow\mathbf{q}-\mathbf{k}} \hat{c}_{\uparrow\mathbf{q}+\mathbf{k}} - \frac{|\Delta|^2}{U} \right). \quad (6)$$

This can be written in matrix form as

$$H = \frac{1}{M} \sum_{\mathbf{k}} \begin{pmatrix} \hat{c}_{\uparrow\mathbf{k}+\mathbf{q}}^\dagger & \hat{c}_{\downarrow-\mathbf{k}+\mathbf{q}} \end{pmatrix} \begin{pmatrix} \epsilon_{\mathbf{k}+\mathbf{q}} - \mu_\uparrow & \Delta \\ \Delta^* & -(\epsilon_{-\mathbf{k}+\mathbf{q}} - \mu_\downarrow) \end{pmatrix} \begin{pmatrix} \hat{c}_{\uparrow\mathbf{q}+\mathbf{k}} \\ \hat{c}_{\downarrow\mathbf{q}-\mathbf{k}}^\dagger \end{pmatrix} + \frac{1}{M} \sum_{\mathbf{k}} \left(\epsilon_{-\mathbf{k}+\mathbf{q}} - \mu_\downarrow - \frac{|\Delta|^2}{U} \right). \quad (7)$$

Because Δ was chosen as the amplitude of the order parameter, it is a real number, which simplifies the expressions. The second sum in (7) is just a constant, but it is important for the calculation of free energies. The eigenvalues of the matrix part (i.e. the quasiparticle energies) are

$$E_{\mathbf{k},\mathbf{q},\pm} = \frac{\mu_\downarrow - \mu_\uparrow}{2} + \frac{\epsilon_{\mathbf{k}+\mathbf{q}} - \epsilon_{-\mathbf{k}+\mathbf{q}}}{2} \pm \sqrt{\left(\frac{\epsilon_{\mathbf{k}+\mathbf{q}} + \epsilon_{-\mathbf{k}+\mathbf{q}}}{2} - \frac{\mu_\downarrow + \mu_\uparrow}{2} \right)^2 + \Delta^2}. \quad (8)$$

With the introduction of the single particle energies $\xi_{\uparrow\mathbf{k}} = \epsilon_{\mathbf{k}} - \mu_\uparrow$ and $\xi_{\downarrow\mathbf{k}} = \epsilon_{\mathbf{k}} - \mu_\downarrow$, this can be written in a simpler form

$$E_{\mathbf{k},\mathbf{q},\pm} = \frac{\xi_{\uparrow\mathbf{k}+\mathbf{q}} - \xi_{\downarrow-\mathbf{k}+\mathbf{q}}}{2} \pm \sqrt{\left(\frac{\xi_{\uparrow\mathbf{k}+\mathbf{q}} + \xi_{\downarrow-\mathbf{k}+\mathbf{q}}}{2} \right)^2 + \Delta^2}. \quad (9)$$

Unequal densities introduce unequal chemical potentials, which destroys the particle-hole symmetry that exists in the standard BCS theory. A suitable Bogoliubov transformation,

$$\begin{pmatrix} \hat{c}_{\uparrow\mathbf{q}+\mathbf{k}} \\ \hat{c}_{\downarrow\mathbf{q}-\mathbf{k}}^\dagger \end{pmatrix} = \begin{pmatrix} u_{\mathbf{k},\mathbf{q}} & v_{\mathbf{k},\mathbf{q}} \\ -v_{\mathbf{k},\mathbf{q}} & u_{\mathbf{k},\mathbf{q}} \end{pmatrix} \begin{pmatrix} \hat{\gamma}_{\uparrow\mathbf{k},\mathbf{q}} \\ \hat{\gamma}_{\downarrow-\mathbf{k},\mathbf{q}}^\dagger \end{pmatrix}, \quad (10)$$

with the coefficients given by

$$u_{\mathbf{k},\mathbf{q}}^2 = \frac{1}{2} \left(1 + \frac{\xi_A}{\sqrt{\xi_A^2 + \Delta^2}} \right), \quad v_{\mathbf{k},\mathbf{q}}^2 = \frac{1}{2} \left(1 - \frac{\xi_A}{\sqrt{\xi_A^2 + \Delta^2}} \right), \quad u_{\mathbf{k},\mathbf{q}} v_{\mathbf{k},\mathbf{q}} = \frac{\Delta}{2\sqrt{\xi_A^2 + \Delta^2}}, \quad (11)$$

where $\xi_A = (\xi_{\uparrow\mathbf{k}+\mathbf{q}} + \xi_{\downarrow-\mathbf{k}+\mathbf{q}})/2$, diagonalizes the Hamiltonian to

$$H = \frac{1}{M} \sum_{\mathbf{k}} \left[\begin{pmatrix} \hat{\gamma}_{\uparrow\mathbf{k},\mathbf{q}}^\dagger & \hat{\gamma}_{\downarrow-\mathbf{k},\mathbf{q}} \end{pmatrix} \begin{pmatrix} E_{\mathbf{k},\mathbf{q},+} & 0 \\ 0 & E_{\mathbf{k},\mathbf{q},-} \end{pmatrix} \begin{pmatrix} \hat{\gamma}_{\uparrow\mathbf{k},\mathbf{q}} \\ \hat{\gamma}_{\downarrow-\mathbf{k},\mathbf{q}}^\dagger \end{pmatrix} + \left(\xi_{\downarrow-\mathbf{k}+\mathbf{q}} - \frac{\Delta^2}{U} \right) \right]. \quad (12)$$

Here, the $\hat{\gamma}_{\sigma,\mathbf{k},\mathbf{q}}$ are the quasiparticle operators and they obey Fermi statistics.

2.1. Self-consistent equations for Δ , μ_\uparrow and μ_\downarrow

The ansatz $U \langle \hat{c}_{\downarrow\mathbf{n}} \hat{c}_{\uparrow\mathbf{n}} \rangle = \Delta e^{2i\mathbf{q}\cdot\mathbf{n}}$ implies $\Delta = U \sum_{\mathbf{k}} \langle \hat{c}_{\downarrow-\mathbf{k}+\mathbf{q}} \hat{c}_{\uparrow\mathbf{k}+\mathbf{q}} \rangle / M$, where M is the total number of lattice sites. With the Bogoliubov transformation (10), this can be written as

$$\begin{aligned} \Delta &= \frac{U}{M} \sum_{\mathbf{k}} \langle \hat{c}_{\downarrow-\mathbf{k}+\mathbf{q}} \hat{c}_{\uparrow\mathbf{k}+\mathbf{q}} \rangle = \frac{U}{M} \sum_{\mathbf{k}} u_{\mathbf{k},\mathbf{q}} v_{\mathbf{k},\mathbf{q}} [f(E_{\mathbf{k},\mathbf{q},-}) - f(E_{\mathbf{k},\mathbf{q},+})] \\ &= \Delta \frac{U}{M} \sum_{\mathbf{k}} \frac{f(E_{\mathbf{k},\mathbf{q},-}) - f(E_{\mathbf{k},\mathbf{q},+})}{2\sqrt{\xi_A^2 + \Delta^2}}. \end{aligned} \quad (13)$$

The following equations hold for the particle numbers

$$N_\uparrow = \sum_{\mathbf{k}} \langle \hat{c}_{\uparrow\mathbf{k}}^\dagger \hat{c}_{\uparrow\mathbf{k}} \rangle = \sum_{\mathbf{k}} u_{\mathbf{k},\mathbf{q}}^2 f(E_{\mathbf{k},\mathbf{q},+}) + v_{\mathbf{k},\mathbf{q}}^2 f(E_{\mathbf{k},\mathbf{q},-}), \quad (14)$$

$$N_\downarrow = \sum_{\mathbf{k}} \langle \hat{c}_{\downarrow\mathbf{k}}^\dagger \hat{c}_{\downarrow\mathbf{k}} \rangle = \sum_{\mathbf{k}} u_{\mathbf{k},\mathbf{q}}^2 f(-E_{\mathbf{k},\mathbf{q},-}) + v_{\mathbf{k},\mathbf{q}}^2 f(-E_{\mathbf{k},\mathbf{q},+}). \quad (15)$$

Equations (13)–(15) are *self-consistent* equations in the sense that they are always satisfied by the stable macroscopic state. In particular, the gap equation, (13), can have many solutions, of which the one with the lowest free energy is stable. For example, for equal populations of the two components, even below the critical temperature, the gap equation always has the trivial solution $\Delta = 0$, in addition to the standard BCS solution. However, the BCS solution has lower free energy and is therefore stable.

It is useful to define a gap function $g(\Delta)$ that vanishes at the correct value of Δ . This reduces (13) to $g(\Delta) = 0$.

$$g(\Delta) = \Delta \frac{U}{M} \sum_{\mathbf{k}} \frac{f(E_{\mathbf{k},\mathbf{q},-}) - f(E_{\mathbf{k},\mathbf{q},+})}{2\sqrt{\xi_A^2 + \Delta^2}} - \Delta = 0. \quad (16)$$

In optical lattices, the relevant quantity, instead of the total number of particles in one component, is the filling fraction of one component. The filling fraction is defined as the number of particles divided by the number of lattice sites. We denote filling fractions as $f_\uparrow = N_\uparrow/M$ and $f_\downarrow = N_\downarrow/M$. Because of the Pauli exclusion principle, only one fermion of each kind can fit on the lowest Hubbard band at each site, thereby having both f_\uparrow and f_\downarrow equal to one means having a full lattice, which is a band insulator. Putting three atoms in the same site or on the same momentum state would mean populating higher energy bands, which involves a significant cost in energy. For superfluidity, the optimum setting, giving the highest value for Δ , is $f_\uparrow = 0.5$ and $f_\downarrow = 0.5$ [43]. For population imbalance, it is useful to define the polarization:

$$P = \frac{f_\uparrow - f_\downarrow}{f_\uparrow + f_\downarrow}. \quad (17)$$

2.2. Experimental parameters

In our numerical calculations, we consider ${}^6\text{Li}$ atoms trapped in a lattice created by $\lambda = 1030$ nm lasers. The wavelength is related to the lattice parameter d by $d = \lambda/2$. The lattice height is $2.5E_R$, where the recoil energy is $\hbar^2(2\pi/\lambda)^2/2m$. In the present paper, calculations are done in zero temperature. Except where explicitly noted, we use -1000 Bohr radii for the scattering length a . Typical lattice sizes we have used are $64 \times 64 \times 64$ and $128 \times 128 \times 128$. We calculate the finite lattice sums explicitly, which limits all the vectors in our numerical analysis to a set of discrete lattice points.

3. Free energy analysis

The relevant free energy of a Fermi gas depends on the physical system in question. We start by considering the grand potential $\Omega = -\frac{1}{\beta} \ln Z_G$, where $Z_G = \text{tr} e^{-\beta H}$, is the partition function of the grand canonical ensemble. The partition function is [44]

$$Z_G = \text{Tr} e^{-\beta H} = \prod_{\mathbf{k}} \left(1 + e^{-\beta \frac{E_{\mathbf{k},\mathbf{q},+}}{M}}\right) \left(1 + e^{\beta \frac{E_{\mathbf{k},\mathbf{q},-}}{M}}\right) e^{-\beta C}, \quad (18)$$

where C corresponds to the constant part of the Hamiltonian and $\beta = 1/k_B T$. The grand potential is

$$\Omega = \frac{1}{M} \sum_{\mathbf{k}} \left[\xi_{\downarrow-\mathbf{k}+\mathbf{q}} + E_{\mathbf{k},\mathbf{q},-} - \frac{\Delta^2}{U} \right] - \frac{1}{\beta} \sum_{\mathbf{k}} \left[\ln \left(1 + e^{-\beta \frac{E_{\mathbf{k},\mathbf{q},+}}{M}}\right) + \ln \left(1 + e^{\beta \frac{E_{\mathbf{k},\mathbf{q},-}}{M}}\right) \right]. \quad (19)$$

At low temperatures, this is independent of β and becomes

$$\Omega = \frac{1}{M} \sum_{\mathbf{k}} \left[\xi_{\downarrow-\mathbf{k}+\mathbf{q}} + E_{\mathbf{k},\mathbf{q},-} - \frac{\Delta^2}{U} + E_{\mathbf{k},\mathbf{q},+} \Theta(-E_{\mathbf{k},\mathbf{q},+}) - E_{\mathbf{k},\mathbf{q},-} \Theta(E_{\mathbf{k},\mathbf{q},-}) \right]. \quad (20)$$

There are two different schemes for treating population imbalanced Fermi gases: fixing the particle numbers or fixing the chemical potentials; this choice depends on the physical system in question. We are interested in the former, but first we will briefly discuss the latter, to enlighten the differences between the two cases.

3.1. Fixed chemical potentials, $\mathbf{q} = 0$

With fixed chemical potentials, the relevant thermodynamic free energy is the grand potential $\Omega(\Delta, \mu_{\uparrow}, \mu_{\downarrow})$. The extrema of Ω , $\partial\Omega/\partial\Delta = 0$, correspond to solutions of the gap equation, (16), i.e. $g(\Delta) = 0$. Figure 1 shows a typical scenario with the chemical potentials fixed at $\mu_{\uparrow} = 0.394$ and $\mu_{\downarrow} = 0.304$. The figure shows how the extrema of Ω coincide with the zeros of $g(\Delta)$. In this scheme, the BP state is unstable because it is a local maximum of $\Omega(\Delta)$. However, both the polarization and the total number of atoms change as Δ changes, as can be seen from figure 2. Therefore the extrema correspond to situations with different total numbers of particles. If the numbers of atoms are to stay fixed in the system, this comparison is not valid.

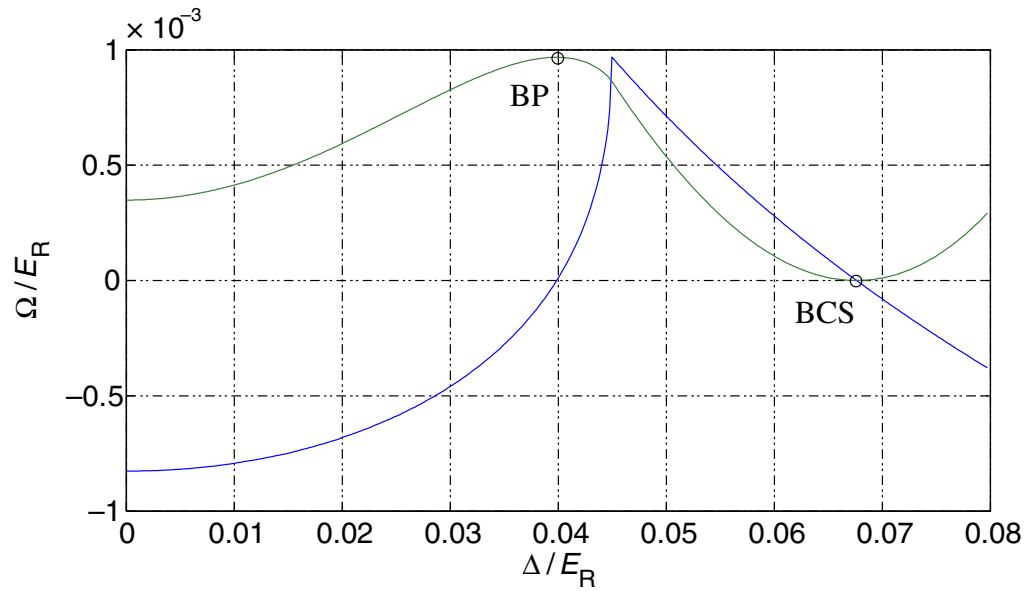


Figure 1. The grand potential Ω per lattice site (green), in the units of recoil energy, and $g(\Delta)/\Delta$ (blue) in arbitrary units. The maximum of Ω at $\Delta = 0.04$ corresponds to the BP state with polarization 0.12, and the minimum at $\Delta = 0.068$ corresponds to the BCS state with a zero polarization. The chemical potentials are fixed at $\mu_{\uparrow} = 0.394$ and $\mu_{\downarrow} = 0.304$.

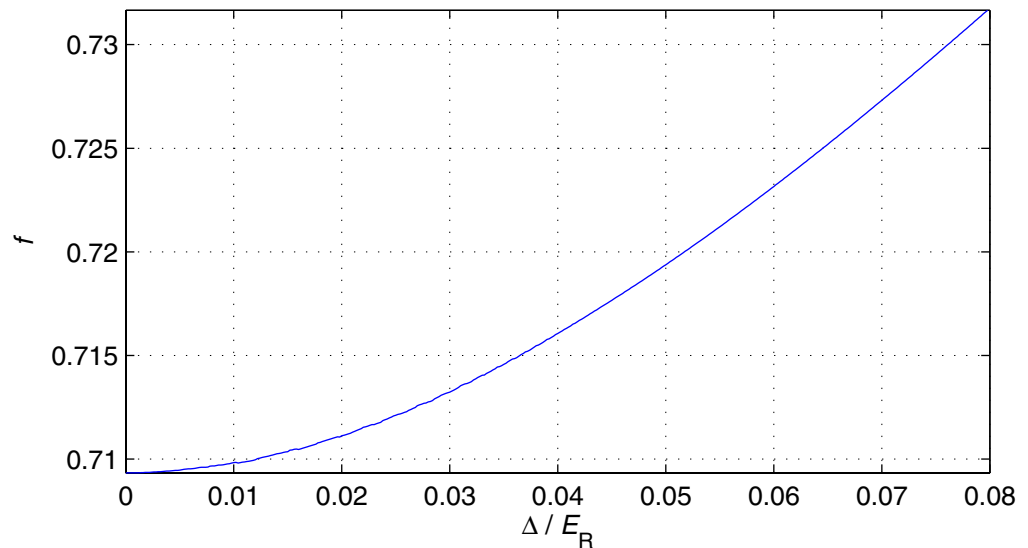


Figure 2. The total filling fraction $f = f_{\uparrow} + f_{\downarrow}$ as a function of Δ , with the chemical potentials fixed at $\mu_{\uparrow} = 0.394$ and $\mu_{\downarrow} = 0.304$.

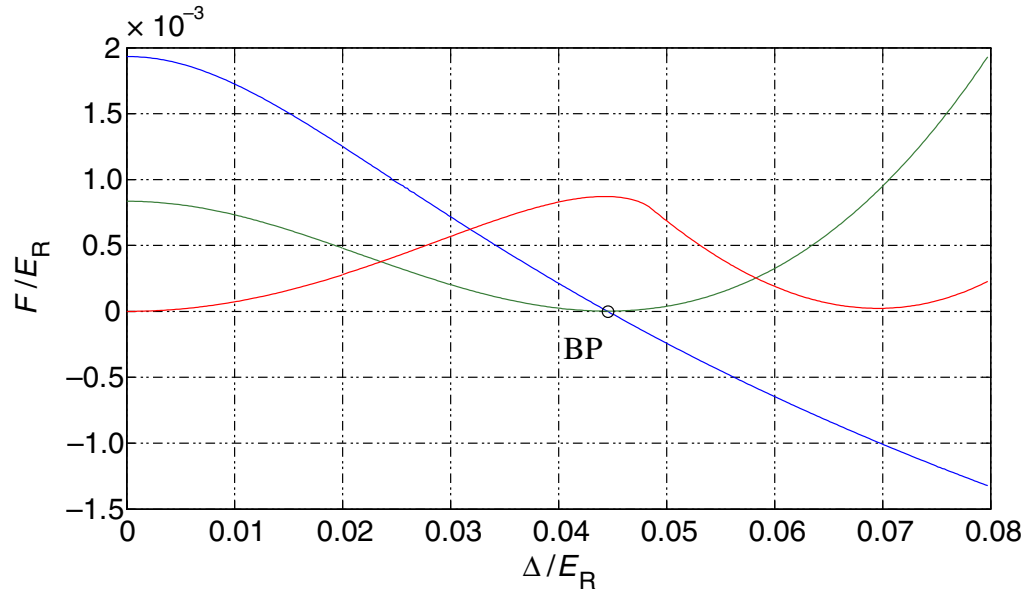


Figure 3. The Helmholtz free energy $F(\Delta)$ per lattice site (green), in the units of recoil energy, and $g(\Delta)/\Delta$ (blue) in arbitrary units. The filling fractions are fixed at $f_{\uparrow} = 0.44$ and $f_{\downarrow} = 0.36$, so the polarization is 0.1. The minimum of F at $\Delta \approx 0.045$, coinciding with the zero of $g(\Delta)$, corresponds to the BP state. Also shown is $\Omega(\Delta)$ (red) with chemical potentials fixed so that the filling fractions have the values mentioned above at the point where $g(\Delta) = 0$.

3.2. Fixed numbers of particles, $\mathbf{q} = 0$

When numbers of particles, instead of the chemical potentials, are fixed, the relevant thermodynamical quantity is the Helmholtz free energy,

$$F(\Delta, N_{\uparrow}, N_{\downarrow}) = \Omega + \mu_{\uparrow} \frac{N_{\uparrow}}{M} + \mu_{\downarrow} \frac{N_{\downarrow}}{M} = \Omega + \mu_{\uparrow} f_{\uparrow} + \mu_{\downarrow} f_{\downarrow}. \quad (21)$$

Now the physical solutions are the minima of $F(\Delta, N_{\uparrow}, N_{\downarrow})$: $\partial F/\partial \Delta = 0$ gives the extrema and $\partial^2 F/\partial \Delta^2 > 0$ defines the minima. These solutions again coincide with the zeros of $g(\Delta)$. Moreover, the extrema given by F are the same as given by Ω , i.e. $\partial \Omega/\partial \Delta = \partial F/\partial \Delta = 0$, but determining which of the extrema are minima, and thereby the physical solutions, depends on whether F or Ω is used. The solutions where \mathbf{q} is fixed at zero are the uniform solutions. If the densities of the different components are the same, the solution is known as the BCS state and if the densities differ, the solution is known as the BP state. With fixed densities, both the BCS ($N_{\uparrow} = N_{\downarrow}$) and the BP ($N_{\uparrow} \neq N_{\downarrow}$) state correspond to a minimum of $F(\Delta)$. We consider there the case $N_{\uparrow} \neq N_{\downarrow}$, that is, the BP state.

Figure 3 shows the Helmholtz free energy and the gap function with fixed numbers of particles (with $N_{\uparrow} \neq N_{\downarrow}$) and \mathbf{q} fixed to 0. It is clear that $F(\Delta)$ is minimized with a finite Δ , i.e. the BP state is stable in this consideration; however one has to consider also the possibility of a nonzero \mathbf{q} .

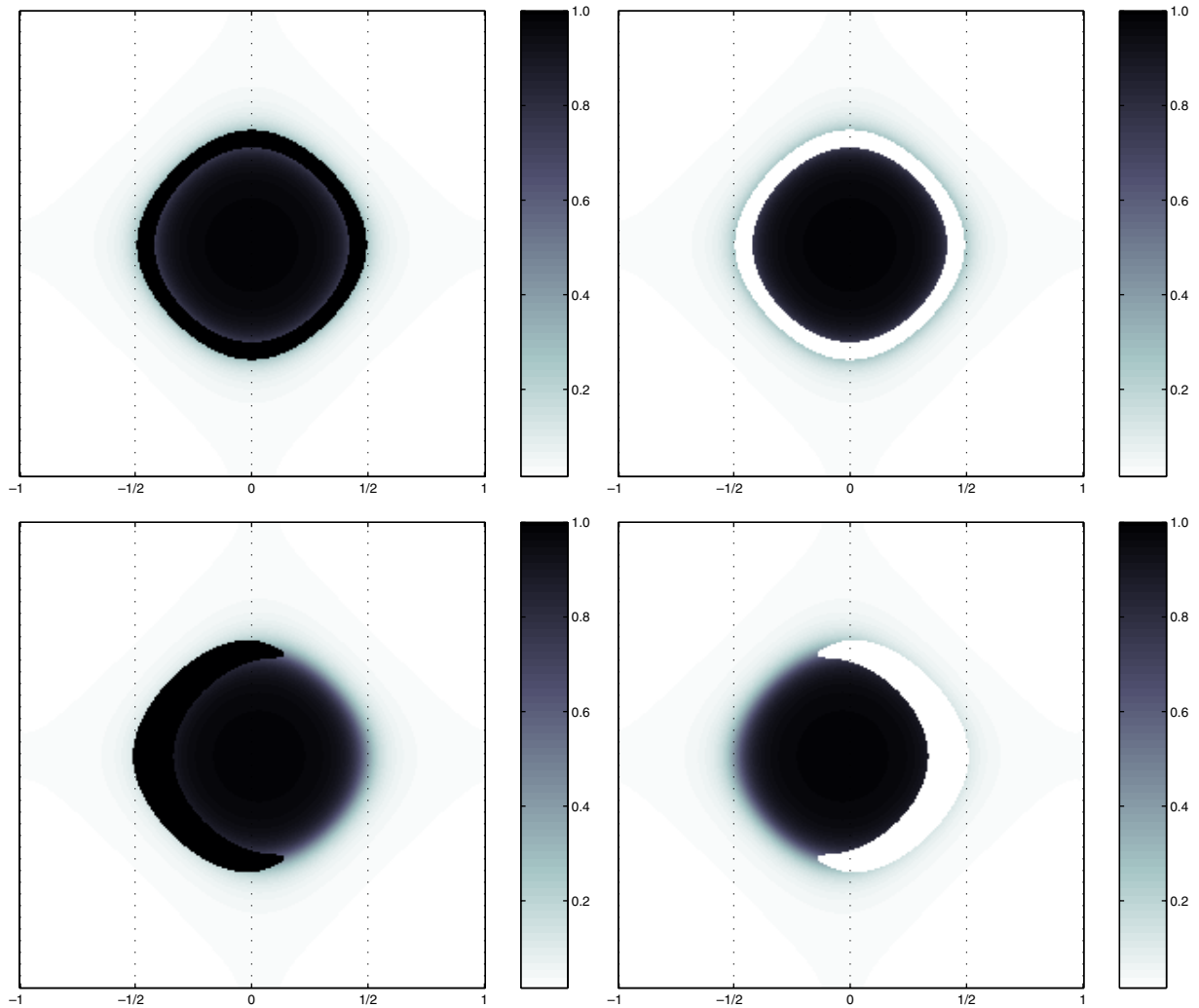


Figure 4. The momentum distributions f_{\uparrow} and f_{\downarrow} , on the $k_z = 0$ plane, of the BP (top row) and FFLO (bottom row) states. Both states demonstrate a depairing region around the Fermi surface, but whereas the region is symmetric in the BP state, it is asymmetric in FFLO. The background scattering length is $-1500a_0$, the total filling fraction is 0.1 and polarization 0.2. In this situation, the FFLO state is energetically favourable.

4. FFLO states

Stability analysis is always limited to some set of states. Many states have been studied in isotropic systems [35, 39, 40], [45]–[47]. A Monte Carlo study [48] suggests the FFLO state to be the ground state in a two dimensional lattice in the weakly interacting regime. Here, we study BCS, BP and single mode FFLO states in three dimensional lattices.

When the particle numbers are fixed and the momentum of the Cooper pairs, $2\mathbf{q}$, is allowed to get nonzero values, the translational symmetry is broken and the state is FFLO like. The stable state is now found by minimizing F with respect to Δ and \mathbf{q} . Figure 4 shows the momentum distributions of the different components along the $k_z = 0$ plane in BP and FFLO states. Note

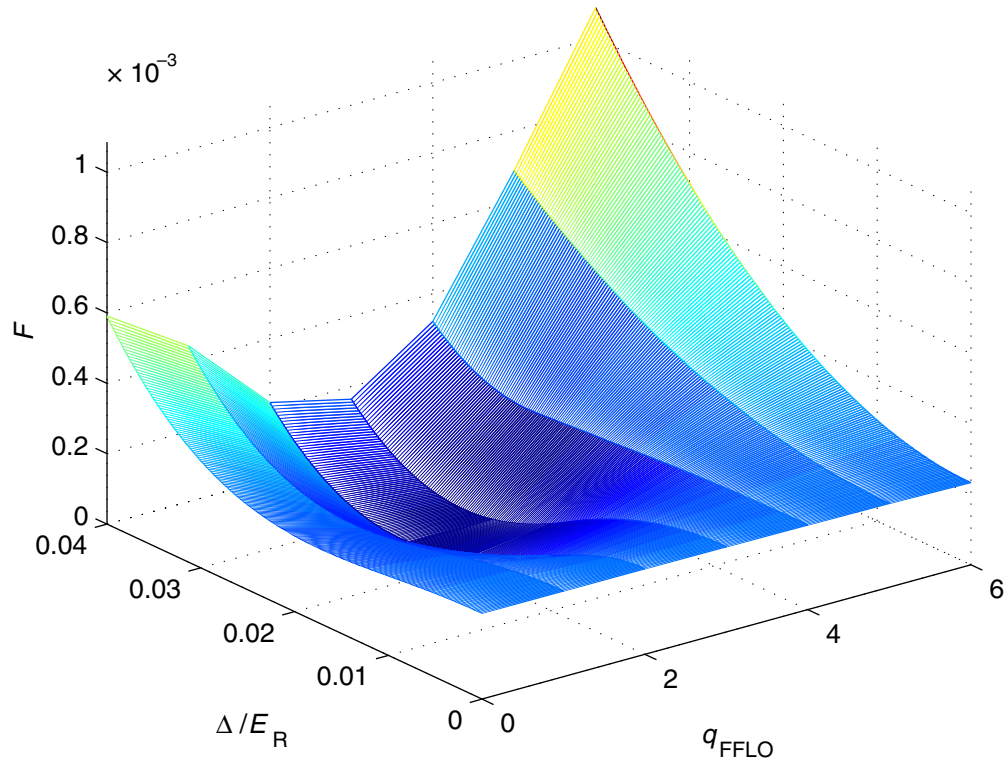


Figure 5. The Helmholtz free energy $F(\Delta, q)$ per lattice site. Here, \mathbf{q} is in the x -direction, i.e. $\mathbf{q} = (q, 0, 0)$. The filling fractions are fixed at $f_{\uparrow} = 0.24$ and $f_{\downarrow} = 0.16$, so that $P = 0.2$. The units of q are selected so that $(32, 32, 32)$ would correspond to the corner of the first Brillouin zone, the R point.

that there is a vacant region, or breach, in the momentum distribution of the minor component in the BP phase.

Figure 5 shows a typical free energy landscape for the FFLO state. The filling fractions are fixed at $f_{\uparrow} = 0.24$ and $f_{\downarrow} = 0.16$. The figure shows that the minimum energy is found with a nonzero Δ and nonzero \mathbf{q} . The BP state is a saddle point and the BCS solution is absent since it does not support polarization at zero temperature.

Figures 6–11 show the energy gap Δ and the FFLO momentum \mathbf{q} as a function of polarization for different interaction strengths. With increasing polarization, the energy gap Δ decreases and the magnitude of \mathbf{q} increases. Whether a critical polarization P_c , where Δ vanishes, exists, depends on the total density $f_{\uparrow} + f_{\downarrow}$ and the interaction strength between the atoms, characterized by the scattering length a . With $a = -1000$ Bohr radii and total filling fractions between 0.4 and 1.0, the critical polarizations are around 0.3. Raising the scattering length to $a = -1500a_0$ gives a P_c around 0.6 with the same densities. With $a = -2000a_0$, P_c is more than 0.9, as can be seen in figure 11.

Figures 6–10 show the $\mathbf{q} = 0$, i.e. the BP phase, with small polarizations. However, the discrete steps in the values of \mathbf{q} are due to the finite size of the lattice and using a larger lattice allows for smaller steps with shorter intervals. We expect these steps, and the kinks in the energy gap, to vanish in the limit of larger lattices. The figures also show that stronger interactions as well as larger densities lead to higher critical polarizations, as is expected.

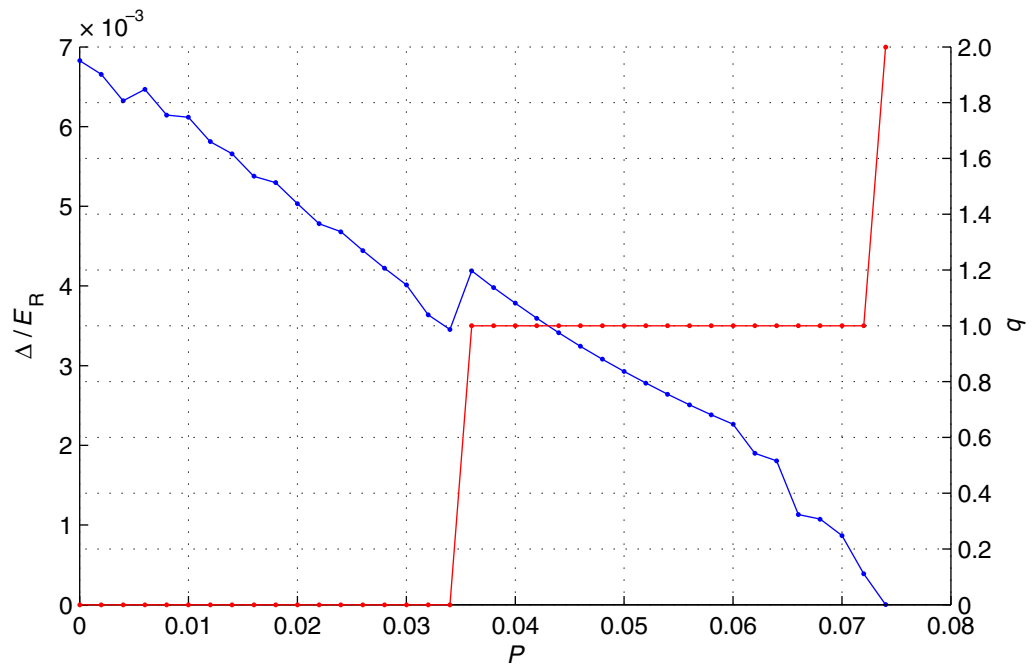


Figure 6. The order parameter Δ (blue) and the magnitude of \mathbf{q} (red) as a function of polarization P . Here, the total filling fraction is 0.1, the scattering length is $-1000a_0$, and the lattice size is $128 \times 128 \times 128$. The q is given in reciprocal lattice indices, so that 64 on the y -axis would correspond to the edge of the first Brillouin zone.

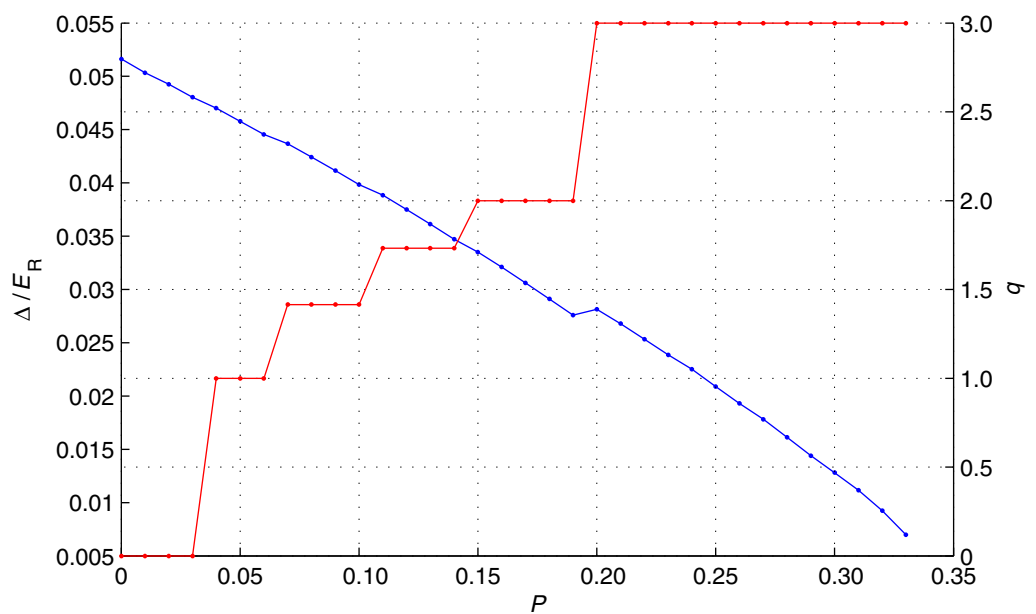


Figure 7. The energy gap Δ and the magnitude of \mathbf{q} as a function of polarization with the total filling fraction of $f = 0.4$ and scattering length $a = -1000a_0$.

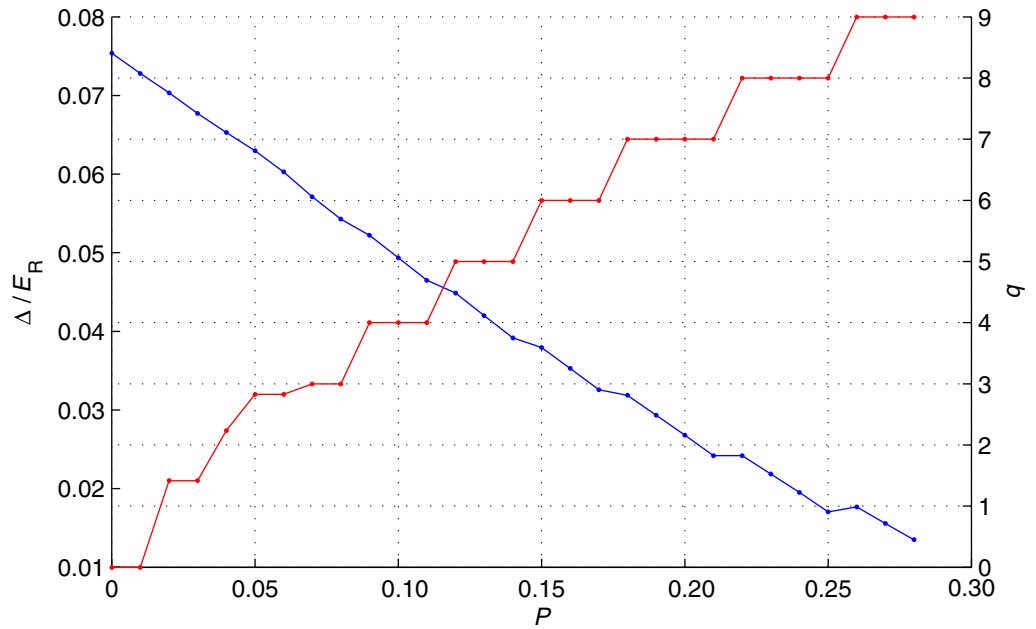


Figure 8. The energy gap Δ and the magnitude of q as a function of polarization with the total filling fraction of $f = 1.0$ and scattering length $a = -1000a_0$.

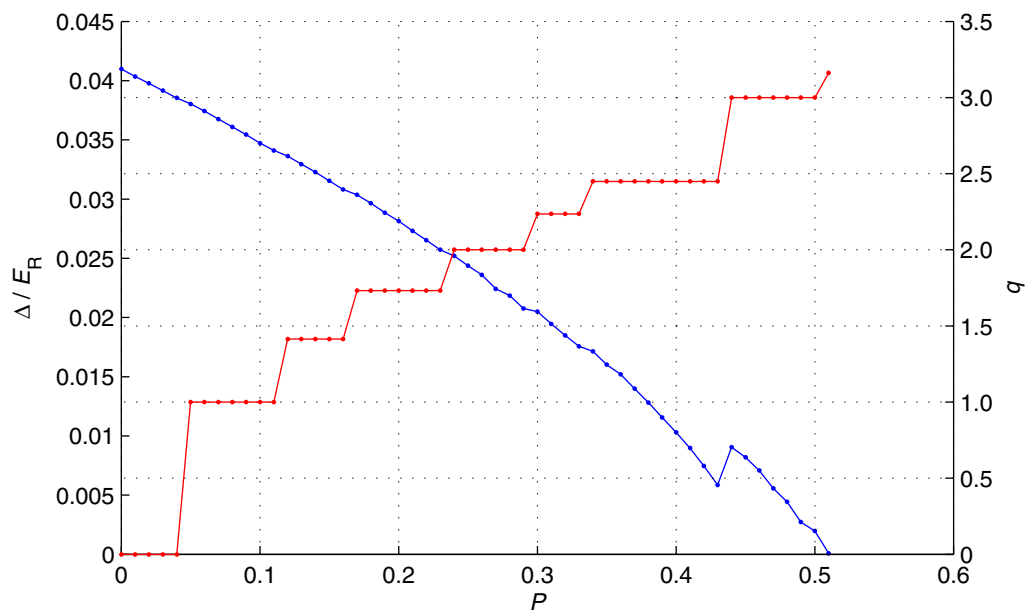


Figure 9. The energy gap Δ and the magnitude of q as a function of polarization with the total filling fraction of $f = 0.1$ and scattering length $a = -1500a_0$.

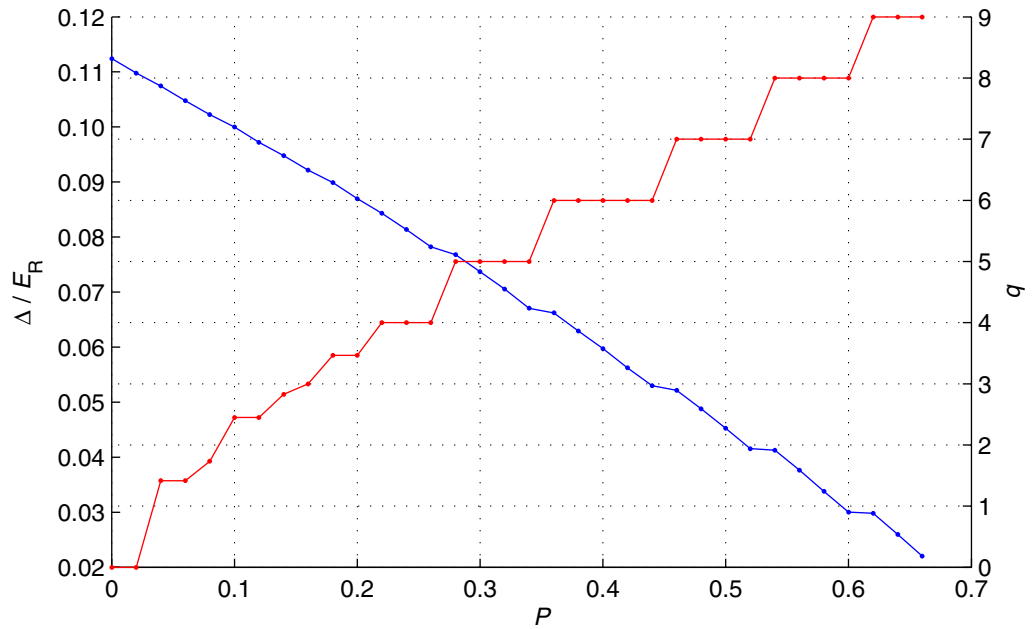


Figure 10. The energy gap Δ and the magnitude of \mathbf{q} as a function of polarization with the total filling fraction of $f = 0.4$ and scattering length $a = -1500a_0$.

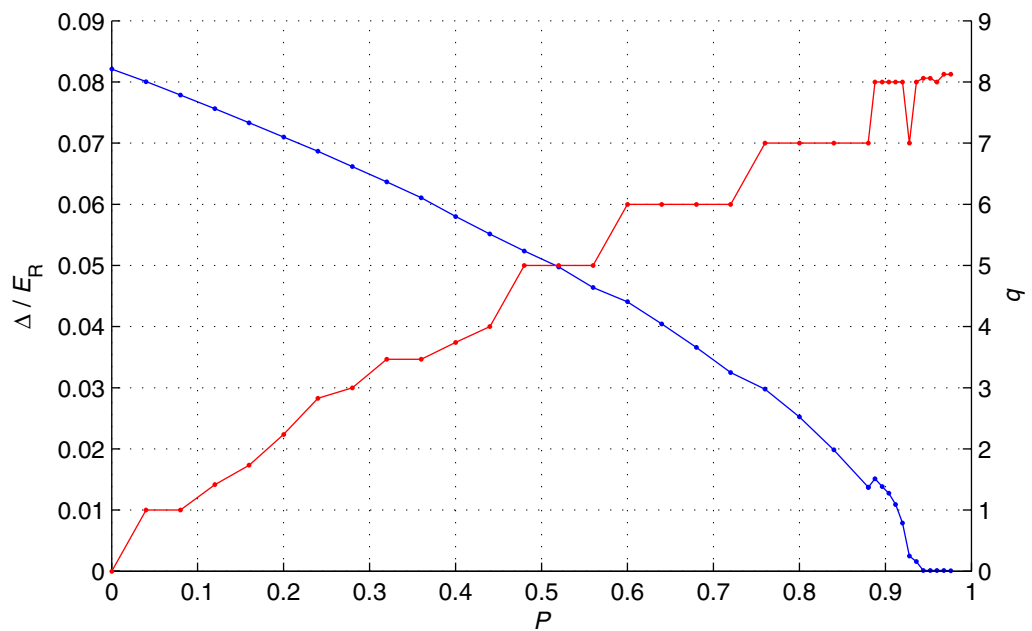


Figure 11. The energy gap Δ and the magnitude of \mathbf{q} as a function of polarization with the total filling fraction of $f = 0.1$ and scattering length $a = -2000a_0$.

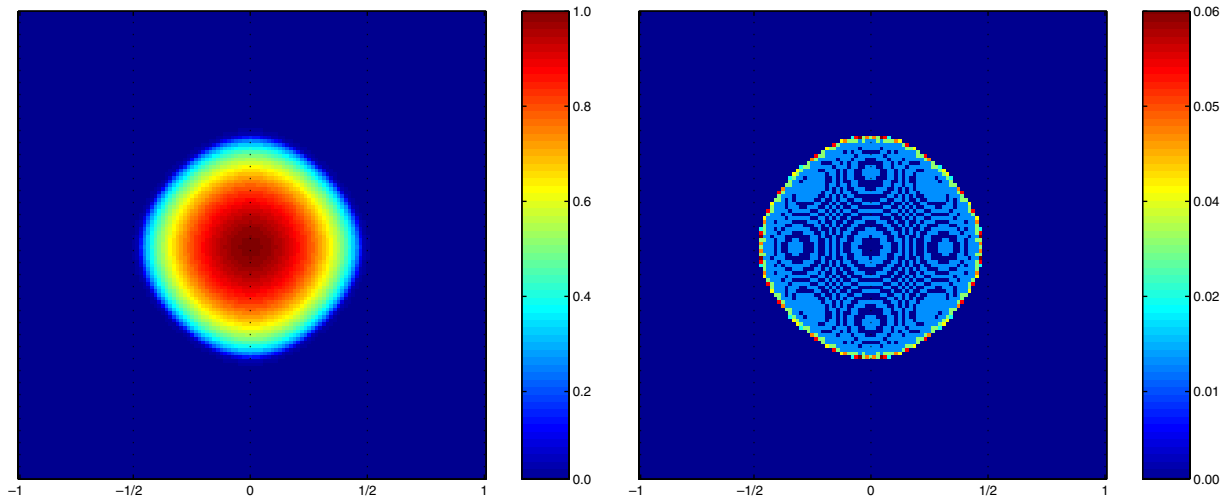


Figure 12. The momentum distributions $f_{\uparrow} + f_{\downarrow}$, and $f_{\uparrow} - f_{\downarrow}$, integrated over the z -direction. Here, the total filling fraction is $f = 0.1$ and $P = 0.02$. Here, $\mathbf{q} = 0$ and the momentum difference shows the BP depairing symmetrically along the Fermi surface.

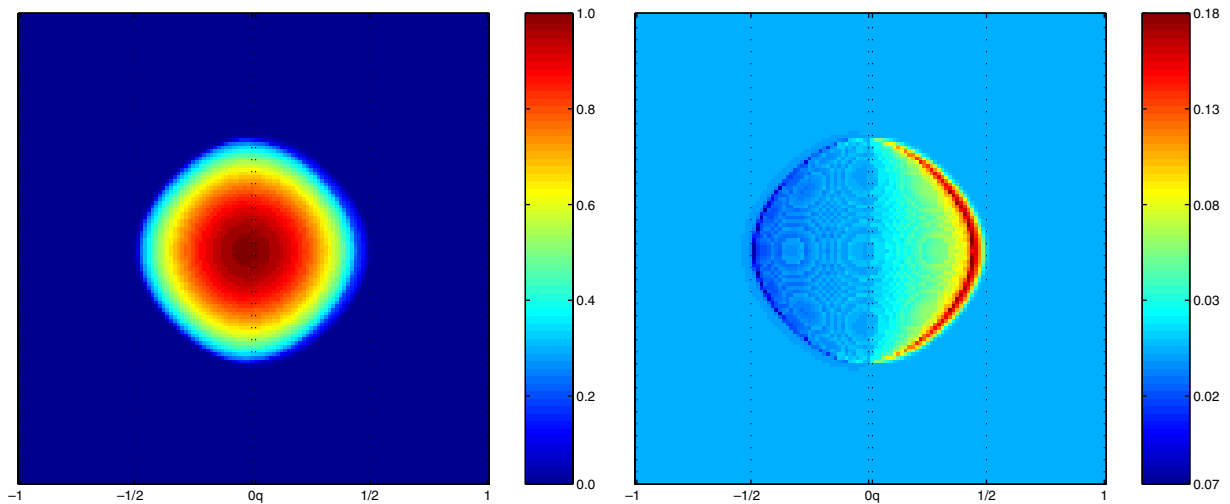


Figure 13. The momentum distributions $f_{\uparrow} + f_{\downarrow}$, and $f_{\uparrow} - f_{\downarrow}$, integrated over the z -direction. Here, the total filling fraction is $f = 0.1$ and $P = 0.04$. The state is of the FFLO type with a finite $q = \pi/(128d)$, which shows clearly in the momentum difference. The depairing region is similar to what has been predicted for homogenous systems, see [49].

Because the Cooper pairs each carry momentum $2\mathbf{q}$, it would seem that the system has total momentum. However, it has been shown for homogenous systems that the net momentum is cancelled by momentum distributions of the individual components cancelling the effect of the momentum q [49]. This is consistent with figures 12–17 where the total momentum distribution $n_k (= f_{\uparrow} + f_{\downarrow})$ is biased to the direction opposite to where q is located. We have also numerically checked that the net momentum is zero.

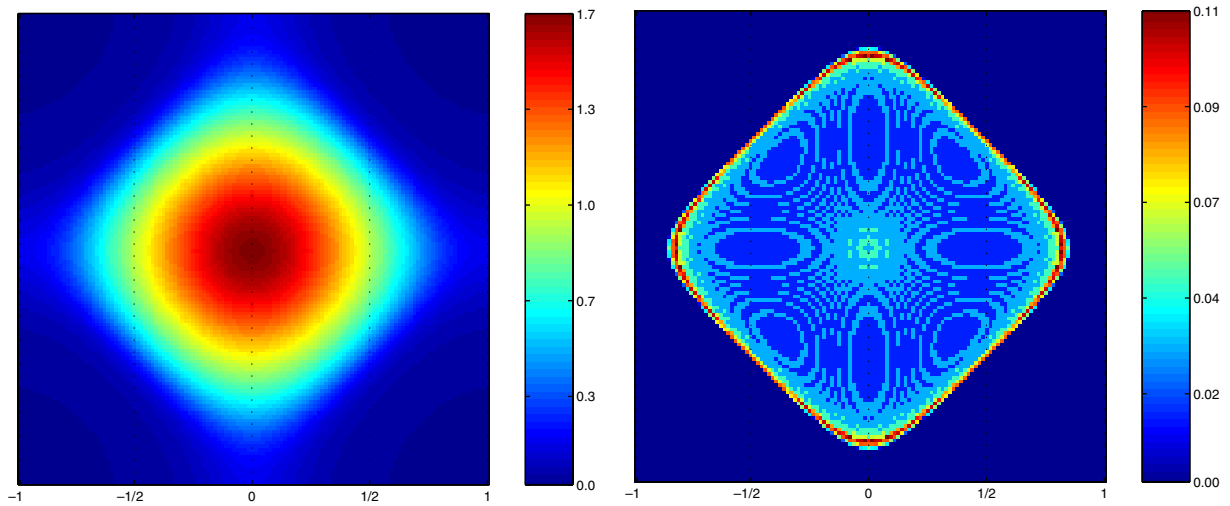


Figure 14. The momentum distributions $f_{\uparrow} + f_{\downarrow}$, and $f_{\uparrow} - f_{\downarrow}$, integrated over the z -direction. Here, the total filling fraction is $f = 0.4$ and $P = 0.03$. Here again $\mathbf{q} = 0$ and the momentum difference shows the BP depairing symmetrically along the Fermi surface.

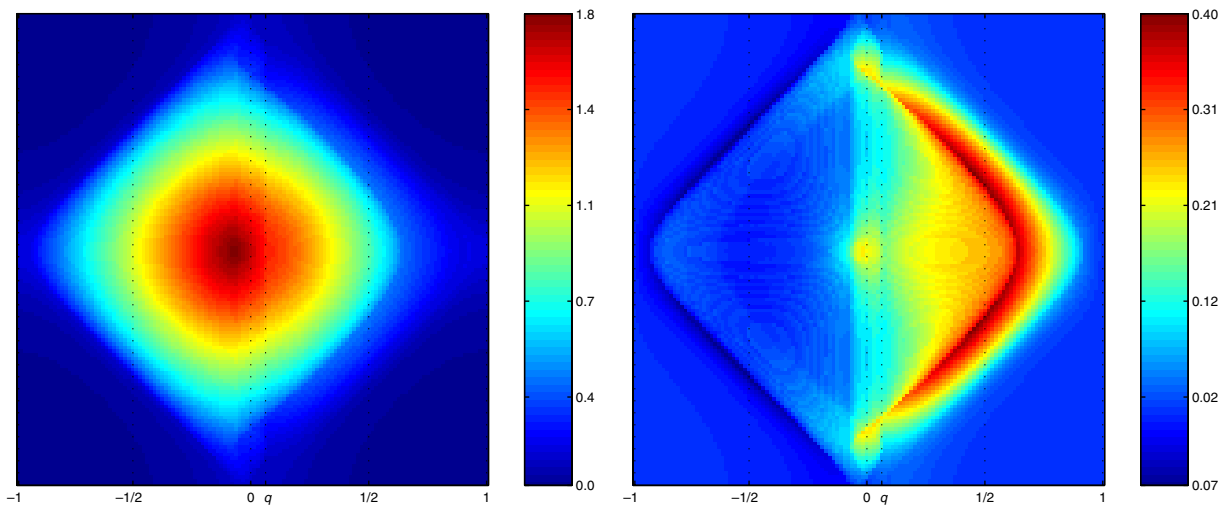


Figure 15. The momentum distributions $f_{\uparrow} + f_{\downarrow}$, and $f_{\uparrow} - f_{\downarrow}$, integrated over the z -direction. Here, the total filling fraction is $f = 0.4$ and $P = 0.15$. The state is FFLO with $q = 2\pi/(64d)$ in the x -direction.

Figures 12–17 show the momentum distributions in different states, integrated over the k_z . The background scattering length is $-1000a_0$ in each figure. The figures show clearly the effect of filling fraction, with low filling fractions giving a spherical Fermi surface, but higher filling fractions showing deformations caused by the lattice. The BP state is visible in the difference of the momentum distributions, $n_{\uparrow\mathbf{k}} - n_{\downarrow\mathbf{k}}$, as a symmetric depairing region, whereas the FFLO phase has asymmetric depairing. Note that the vacant region in the momentum distribution in

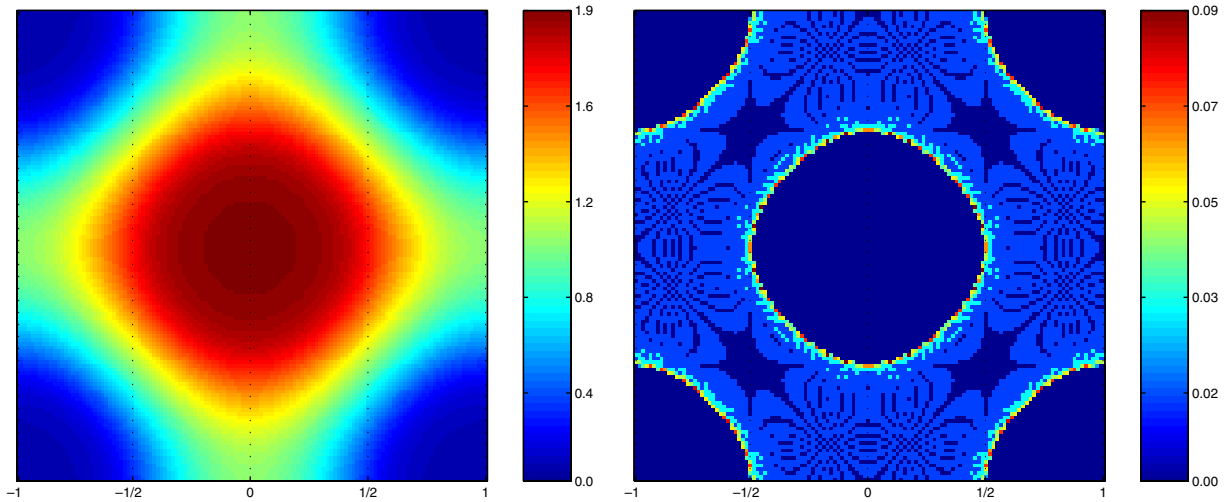


Figure 16. The momentum distributions $f_{\uparrow} + f_{\downarrow}$, and $f_{\uparrow} - f_{\downarrow}$, integrated over the z -direction. Here, the total filling fraction is $f = 1.0$ and $P = 0.01$ and the state is BP.

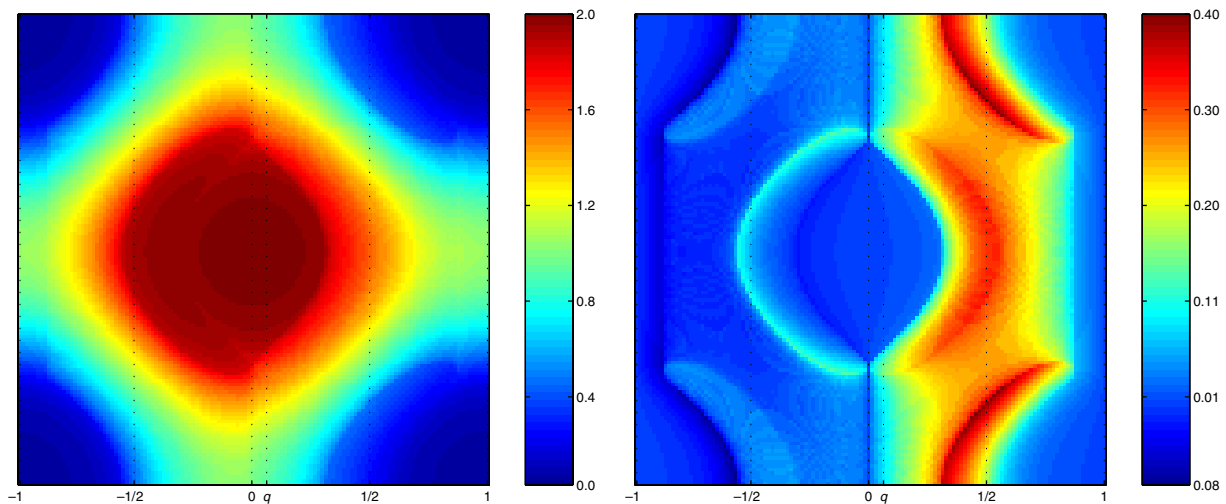


Figure 17. The momentum distributions $f_{\uparrow} + f_{\downarrow}$, and $f_{\uparrow} - f_{\downarrow}$, integrated over the z -direction. Here, the total filling fraction is $f = 1.0$ and $P = 0.08$ and the state is FFLO with $q = 2\pi/(64d)$ in the x -direction.

the BP phase is present, but not visible due to the column integration and also due to the small polarization.

The FFLO state has been suggested to be observable in the correlations in the atom shot noise [50]; however, as figures 12–17 show, the FFLO state is already reflected in the momentum distributions.

5. Conclusions

We have shown that, in the case of interacting fermionic atoms trapped in optical lattices, a stable FFLO state can be found. The stability of various non-BCS superfluids such as BP state/Sarma state has been an intriguing topic of study and it is known that the stability depends for instance on whether the particle number in the system is fixed or not. Moreover, one has to always consider also the possibility of a state beyond the BP/Sarma state, such as FFLO-type states associated with a nonzero Cooper pair momentum. The FFLO state has been predicted to lower the system free energy compared to the BP state in many cases; however, it is often predicted to occur only in some narrow parameter window [39, 40]. According to the analyses we present here, in atomic gases trapped in optical lattices, the FFLO state minimizes the relevant free energy, and does it for a considerable range of parameters. This is influenced by the fact that the particle numbers, not the chemical potentials, are fixed in trapped atomic gases. Furthermore, considerable critical polarizations can be achieved, which may be partly aided by lattice features. For low filling fractions, e.g. $f = 0.1$, critical polarizations are $P_c = 0.075$, 0.5 and 0.9 for the scattering lengths $-1000a_0$, $-1500a_0$ and $-2000a_0$, respectively, showing strong dependence on the interactions. Also raising the filling fraction increases the critical polarization, for instance for $-1000a_0$ scattering length, $P_c = 0.3$ for $f = 0.4$ (compared to $P_c = 0.075$ for $f = 0.1$). Interestingly, however, further increase of f does not necessarily make P_c to grow, for example $P_c = 0.3$ also for $f = 1$. This dependence of the critical polarization on the filling fraction requires further study and may be useful in comparison of theory to experiments. Stronger interactions may bring in additional interesting features, but then one has to consider the validity of the single band approximation. We have also showed that the FFLO state is clearly reflected in the directly observable momentum distribution of the atoms.

An important topic of further study is to evaluate the effect of the residual harmonic trapping potential which is always associated with optical lattices, despite their approximate periodic translational invariance. Issues related to potential phase separation have to be clarified. Based on previous experiments on bosonic and fermionic atoms in optical lattices, it seems possible to limit the effect of the harmonic potential in such a way that essential predictions of a homogeneous lattice model can be observed. On the other hand, for strong harmonic trapping, interesting combined lattice and phase separation effects may be seen.

Acknowledgments

This work was supported by the Finnish Cultural Foundation, the Academy of Finland, and EUROHORCs (EURYI, Academy projects nos. 106299, 205470 and 207083).

References

- [1] Jochim S *et al* 2003 *Science* **302** 2101
- [2] Regal C, Greiner M and Jin D 2003 *Nature* **426** 537
- [3] Regal C, Greiner M and Jin D 2004 *Phys. Rev. Lett.* **92** 040403
- [4] Zwierlein M W *et al* 2004 *Phys. Rev. Lett.* **92** 120403
- [5] Bartenstein M *et al* 2004 *Phys. Rev. Lett.* **92** 203201
- [6] Kinast J, Hemmer S L, Gehm M E, Turlapov A and Thomas J E 2004 *Phys. Rev. Lett.* **92** 150402
- [7] Chin C *et al* 2004 *Science* **305** 1128

- [8] Kinast J *et al* 2005 *Science* **307** 1296
- [9] Zwierlein M W, Abo-Shaeer J, Schirotzek A, Schunck C and Ketterle W 2005 *Nature* **435** 1047
- [10] Zwierlein M W, Schirotzek A, Schunck C H and Ketterle W 2006 *Science* **311** 492
- [11] Partridge G B, Li W, Kamar R I, Liao Y and Hulet R G 2006 *Science* **311** 503
- [12] Zwierlein M W and Ketterle W 2006 *Preprint cond-mat/0603489*
- [13] Sheehy D E and Radzihovsky L 2006 *Phys. Rev. Lett.* **96** 060401
- [14] Pieri P and Strinati G 2006 *Phys. Rev. Lett.* **96** 150404
- [15] Kinnunen J, Jensen L M and Törmä P 2006 *Phys. Rev. Lett.* **96** 110403
- [16] Yi W and Duan L-M 2006 *Phys. Rev. A* **73** 034307
- [17] Chevy F 2006 *Phys. Rev. Lett.* **96** 130201
- [18] He L, Jin M and Zhuang P 2006 *Phys. Rev. B* **73** 214527 (*Preprint cond-mat/0601147*)
- [19] Silva T N D and Mueller E J 2006 *Phys. Rev. A* **73** 051602 (R) (*Preprint cond-mat/0601314*)
- [20] Haque M and Stoof H 2006 *Preprint cond-mat/0601321*
- [21] Ho T-L and Zhai H 2006 *Preprint cond-mat/0602568*
- [22] Bulgac A, Forbes M M and Schwenk A 2006 *Phys. Rev. Lett.* **97** 020402 (*Preprint cond-mat/0602274*)
- [23] Machida K, Mizushima T and Ichioka M 2006 *Preprint cond-mat/0604339*
- [24] Jensen L M, Kinnunen J and Törmä P 2006 *Preprint cond-mat/0604424*
- [25] Silva T N D and Mueller E J 2006 *Preprint cond-mat/0604638*
- [26] Imambekov A, Bolech C J, Lukin M and Demler E 2006 *Preprint cond-mat/0604423*
- [27] Casalbuoni R and Nardulli G 2004 *Rev. Mod. Phys.* **76** 263
- [28] Greiner M, Mandel O, Esslinger T, Hänsch T W and Bloch I 2002 *Nature* **415** 39
- [29] Modugno G, Ferlaino F, Heidemann R, Roati G and Inguscio M 2003 *Phys. Rev. A* **68** 011601
- [30] Pezze L *et al* 2003 *Phys. Rev. Lett.* **93** 120401
- [31] Köhl M, Moritz H, Stöferle T, Günter K and Esslinger T 2005 *Phys. Rev. Lett.* **94** 080403
- [32] Stöferle T, Moritz H, Günter K, Köhl M and Esslinger T 2006 *Phys. Rev. Lett.* **96** 030401 (*Preprint cond-mat/0509211*)
- [33] Stöferle T *et al* 2005 Fermionic atoms with tunable interactions in a 3d optical lattice *Proc. 17 Int. Conf. on Laser Spectroscopy* (Singapore: World Scientific) p 283 (*Preprint cond-mat/0601045*)
- [34] Günter K, Stöferle T, Moritz H, Köhl M and Esslinger T 2006 *Phys. Rev. Lett.* **96** 180402 (*Preprint cond-mat/0604139*)
- [35] Sarma G 2003 *J. Phys. Chem.* **24** 1029
- [36] Liu W V and Wilczek F 2003 *Phys. Rev. Lett.* **90** 047002
- [37] Liu W V, Wilczek F and Zoller P 2004 *Phys. Rev. A* **70** 033603
- [38] Forbes M M, Gubankova E, Liu W V and Wilczek F 2005 *Phys. Rev. Lett.* **94** 017001
- [39] Fulde P and Ferrell R A 1964 *Phys. Rev. A* **135** 550
- [40] Larkin A I and Ovchinnikov Y N 1965 *Sov. Phys.—JETP* **20** 762
- [41] Jaksch D, Bruder C, Cirac J, Gardiner C W and Zoller P 1998 *Phys. Rev. Lett.* **81** 3108
- [42] Koponen T, Martikainen J-P, Kinnunen J and Törmä P 2006 *Phys. Rev. A* **73** 033620
- [43] Micnas R, Ranninger J and Robaszkiewicz S 1990 *Rev. Mod. Phys.* **62** 113
- [44] Fetter A L and Walecka J D 2003 *Quantum Theory of Many-Particle Systems* (New York: Dover)
- [45] Machida K and Nakanishi H 1984 *Phys. Rev. B* **30** 122
- [46] Bedaque P F, Caldas H and Rupak G 2003 *Phys. Rev. Lett.* **91** 247002
- [47] Sedrakian A, Mur-Petit J, Polls A and Muther H 2005 *Phys. Rev. A* **72** 013613
- [48] Dukelsky J, Ortiz G, Rombouts S M A and Houcke K V 2006 *Phys. Rev. Lett.* **96** 180404
- [49] Takada S and Izuyama T 1969 *Prog. Theor. Phys.* **41** 635
- [50] Yang K 2005 *Phys. Rev. Lett.* **95** 218903